

XU, S., REN, J., LU, H., WANG, X., SUN, X. and LIANG, X. 2022. Nondestructive detection and grading of flesh translucency in pineapples with visible and near-infrared spectroscopy. *Postharvest biology and technology* [online], 192, article 112029. Available from: <https://doi.org/10.1016/j.postharvbio.2022.112029>

Nondestructive detection and grading of flesh translucency in pineapples with visible and near-infrared spectroscopy.

XU, S., REN, J., LU, H., WANG, X., SUN, X. and LIANG, X.

2022

© 2022 Elsevier B.V.

1 **Nondestructive Detection and Grading of Flesh Translucency in Pineapples with Visible**
2 **and Near-infrared Spectroscopy**

3 Sai Xu^{a,b}, Jinchang Ren^{d*}, Huazhong Lu^{a,b*}, Xu Wang^c, Xiuxiu Sun^e, Xin Liang^{a,b}

4 a. Institute of Facility Agriculture of Guangdong Academy of Agricultural Sciences,
5 Guangzhou 510640, China

6 b. Guangdong Laboratory for Lingnan Modern Agriculture, Guangzhou 510640, China

7 c. Institute of Quality Standard and Monitoring Technology for Agro-Products of Guangdong
8 Academy of Agricultural Sciences, Guangzhou 510640, China

9 d. National Subsea Centre, Robert Gordon University, Aberdeen, AB21 0BH, U.K.

10 e. USDA, Agricultural Research Service, US Pacific Basin Agricultural Research Center, 64
11 Nowelo Street, Hilo, HI, 96720, USA

12 * Corresponding author: Huazhong Lu (huazlu@scau.edu.cn), Jinchang Ren
13 (Jinchang.Ren@ieee.org)

14
15 **Abstract:** Rapid, accurate, and nondestructive internal quality detection for large and rough
16 surface fruit, such as translucency in pineapples, is challenging. In this paper, a visible and near
17 infrared (VIS/NIR) spectrum-based platform is proposed for optimized detection of pineapple
18 translucency. The internal quality of three batches of samples harvested at the same maturity
19 but on different dates (early, middle, and mid to late harvest stage) were acquired with different
20 spectral settings: VIS to shortwave NIR (400-1100 nm), NIR (900-1700 nm) and VIS/NIR
21 (400-1700 nm). The pineapple samples were manually cut open and divided into three

22 translucency degrees (no, slight, and heavy), according to marketing standards. The Savitzky
23 Golay (SG) and standard normal variate (SNV) were applied to remove jitter and scattering
24 noise, respectively. The successive projections algorithm, principal component analysis and
25 Euclidean distance were combined for feature extraction and measurement, followed by data
26 modeling using the partial least squares regression and probabilistic neural network (PNN).
27 Data correction, data supplementation, and a combination of these were applied for model updating.
28 Experimental results showed that the optimal solution for pineapple translucency detection was to
29 use 400-1100 nm spectrum with SG, SNV, PNN and data supplementation for model
30 updating. With only the first and second batch of samples used for modeling (validation set
31 accuracy 91.2 %) and updating (validation set accuracy 100 %), the detection accuracy on the
32 third batch samples was 100 %. The proposed methodologies therefore can be used as
33 rapid, nondestructive, and cost-effective tools to detect pineapple translucency to guarantee
34 the marketing of high-quality fruit, which can also guide the postharvest treatment for
35 the pineapple industry to improve market competitiveness as well as to benefit nondestructive
36 quality assessment of other large fruit.

37 **Keywords:** Pineapple; translucency; visible and near infrared spectroscopy; nondestructive
38 detection

40

41

42

43 **1. Introduction**

44 Pineapple is one of the most economically important crops in tropical and subtropical areas,
45 however, for the past several decades, it has been damaged by flesh translucency (Paull and
46 Reyes, 1996). Pineapple flesh translucency (PFT) is an irreversible physiological disorder,
47 which affects the flesh and results in low porosity, a water soaked appearance, flat and over-
48 ripe off flavor, rotten taste, and much lower edible quality (Chen and Paull, 2000).
49 Translucent fruit are very susceptible to damage after mechanical collision during transportation
50 and may decay fast during storage (Py et al., 1987). PFT can be caused by either natural or
51 human factors such as pre-harvest temperature, sunburn, excessive rainfall, and
52 overfertilization (Cano Reinoso, 2021; Chen, 1999; Murai et al., 2021; Paull and Chen, 2013).
53 Despite various efforts by researchers and farmers, PFT remains a frequent occurrence at
54 present.

55 PFT occurs in many countries around the world, such as Benin, Brazil, China, Costa Rica,
56 India, Nigeria, Thailand, USA, etc, and the occurrence rate can reach 87.77% with poor-
57 management (Adetunji et al., 2012; Chen and Paull, 2000; Fassinou Hotegni et al., 2014;
58 Korres et al., 2010; Mandal and Vanlalawmpuia, 2020; Montero-Calderón et al., 2008;
59 Joomwong and Sornsrivichai, 2006). According to the investigation, the PFT occurrence rates
60 in Zhanjiang, the largest producing area of China, were 15 %, 24 %, and 44 % annually from
61 2019 to 2021. The increasing PFT rate requires the urgent attention of researchers. In China,
62 pineapple is mainly planted by individual farmers without a unified planting standard that
63 makes the control and treatment of PFT even harder in the short term. Thus, it is crucial to

64 explore a nondestructive, fast, and smart solution for PFT detection and grading in order to
65 determine the most suitable postharvest treatments to maintain market quality, protect the brand,
66 and improve market competitiveness.

67 In the past, acoustic detection was widely applied in industry by knocking the pineapple
68 manually, where a duller sound indicated a more serious degree of translucency. However, the
69 accuracy of acoustic detection is only about 60%, and is also labor intensive and inefficient.
70 Although acoustic impulse-response technique was found feasible for fruit internal quality
71 assessment (Duprat et al., 1997), this technique has not been extensively used by the industry
72 due to its sensitivity to the environmental noise. Haff et al. proposed an X-ray image method
73 for the detection of pineapple translucency, where the detection accuracies for no translucency
74 and extreme translucency were 95 % and 85 %, respectively (Haff et al., 2006). However,
75 X-ray technology has a high cost, is a radiological hazard and is slow, which makes it hard for
76 the agro-product industry to adopt. Therefore, exploration of nondestructive, fast, and
77 cost-effective methods for pineapple translucency detection is still vital and remains unsolved.

78 Recently, visible and near infrared (VIS/NIR) spectroscopy (Pahlawan et al., 2021),
79 electronic nose (Shi et al., 2018), and machine vision (Naik and Patel, 2017) techniques have
80 become mainstream technologies in nondestructive quality assessment of agro-products. As the
81 occurrence of translucency starts from the heart of the pineapple before spreading out to the
82 whole flesh, electronic nose and machine vision fail to characterize the translucency position of
83 pineapple directly due to the fact that they rely mainly on superficial features such as
84 volatile, color, shape, and size. VIS/NIR spectrum, the previous experiment found, is able to

85 transmit the whole pineapple with enough light intensity and quickly acquire abundant
86 information about the internal quality, which is more suitable for pineapple translucency
87 detection than other technologies (Xu et al., 2021). Additionally, the successful and
88 nondestructive detection of the internal quality of watermelon (Jie and Xuan, 2018) and
89 pomelo (Xu et al., 2020) was demonstrated using the VIS/NIR transmission spectra. However,
90 the nondestructive detection of the internal quality of large fruit is rarely reported.
91 Translucency starts from the middle of the pineapple, which requires an acquired spectrum
92 with a higher signal to noise ratio. Thus, further research on pineapple is still needed due to
93 its unique characteristics.

94 VIS/NIR spectroscopy has been successfully applied to a wide range of internal quality
95 assessment tasks, such as total soluble solids content, acidity, firmness, pathology, and insect
96 infestation (Adedeji et al., 2020; Li et al., 2016; Lu et al., 2020; Wang et al., 2015), especially
97 for small fruits, such as apple, pear, peach, and kiwi. However, the large size and rough skin of
98 pineapple can easily increase the scattered noise of the spectral signal, leading to difficulty
99 in detecting the internal quality compared to other small fruit. Whether pineapple
100 translucency can be detected using the VIS/NIR spectroscopy or not is still an open question.
101 In addition, most of the existing works focus on nondestructive detection in a lab based setting,
102 where the application cost and model adaptation among different batches of samples are often
103 ignored (Cruz et al., 2021; Zhang et al., 2021). As detection cost and model robustness are two
104 important factors for the potential deployment of the developed techniques in real industrial
105 applications, they need be addressed accordingly.

106 To tackle these challenging issues, the objectives of the work were to (1) test the efficiency
 107 of nondestructive pineapple translucency detection using a developed VIS/NIR spectroscopy-
 108 based method; (2) balance the detection accuracy and the cost using two spectroscopies in
 109 different wavelengths; (3) explore the robustness of the detection model by using three batches
 110 of pineapple samples harvested at different times, one for training, one for updating, and the
 120 other for testing in practical applications.

121 2.1. Pineapple samples

122 The experimental pineapple samples, variety ‘Bali’, were harvested at Youhao farmland in
 123 Zhanjiang, Guangdong Province, China. Three batches of pineapple samples were harvested at
 124 different dates for model training, updating, and testing (Table 1). All samples were harvested
 125 at the same maturity and, with the same cultivation pattern, although they were planted at
 126 different dates. Pineapple sampling was conducted in a temporary laboratory near the farmland.
 127 For data sampling of the third batch, 10, 20, 20, 20, and 20 samples were used on different
 128 postharvest times.

129 Table 1 Experimental pineapple sample information

Batch	Sample size	Harvest / sampling date	Data use and data splitting of cross validation
1	100	Both on 16 th , April, 2021	(1) Model training: 67 samples (38, 14, and 15 samples were randomly selected from the three categories of no, slight, and heavy translucency,

			respectively) for calibration, the rest 34 samples of batch 1 for validation;
2	100	Both on 1 st , May, 2021	(2) Necessity test of model updating: Whole batch 1 for calibration, and whole batch 2 for validation;
3	90	3 rd , May, 2021 / 3 rd , 5 th , 7 th , 9 th , 11 th May, 2021	(3) Model updating: Whole batch 1 plus part (gradually increased) of batch 2 for calibration, the rest of batch 2 for validation; (4) Model testing: Whole batch 1 and part (gradually increased) of batch 2 for calibration, whole batch 3 for validation.

130

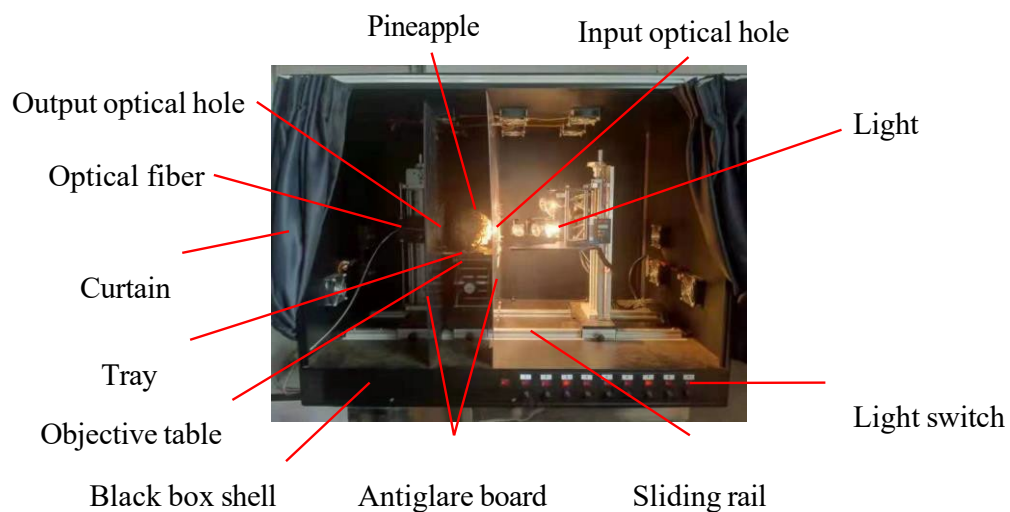
131 2.2. VIS/NIR based spectrum detection

132 The lab-based VIS/NIR spectrum detection platform for pineapple internal quality inspection
133 is shown in Figure 1. In consideration of practical requirements of stability of pineapple samples
134 on the assembly line, each pineapple fruit is put on a tray when being imaged. To avoid
135 scattering noise being received by the optical fiber, all light goes through both the input and
136 output optical holes, passing through the pineapple fruit, before being detected by the optical
137 fiber. The whole sampling process was conducted in a dark environment composed of a black
138 box and curtain.

139 For optimal sampling effect, all the key parameters of the platform were adjustable. The
140 light source is composed of 9 halogen lamps (the power is 100 W each, LM-100, MORITEX
141 Company, Japan), the power of the whole lighting system varies from 100 W to 900 W. The
142 sizes of the input and output optical holes can be determined empirically by changing and
143 testing for multiple times. The distance among the light, pineapple, and optical fiber can also
144 be adjusted by moving components on a sliding rail. In addition, there are only two kinds of

145 commonly used VIS/NIR spectroscopy sensors on the market, namely 400-1100 nm, and 900-
146 1700 nm. Thus, another end of the optical fiber is connected to two different modularized spectro-
147 scopy sensors: QE PRO (400-1100 nm) and NIR QUEST (900-1700 nm), both produced by the
148 Ocean Optics Company, USA. The combination of these two can cover 400-1700 nm
149 wavelengths.

150 After testing repeatedly, the key parameters of the VIS/NIR spectrum detection platform
151 for pineapple inspection were set as follows. The integral times of QE PRO and NIR QUEST
152 were 600 ms and 2000 ms, respectively. The distance between the optical fiber and the tray was
153 30 mm. The distance between the light and the input optical hole was 84 mm. The power of the
154 light source was 500 W. The pineapple sample was put in the groove in the middle of the tray.
155 The light source, input optical hole, pineapple, output optical hole, and optical fiber were all at
156 the same horizontal level. Under the parameters of the lab-developed VIS/NIR platform, the
157 light would only project onto the pineapple fruit body, before being received by spectroscopy
158 sensors.



163

164 **Fig. 1.** Structure of lab-developed VIS/NIR spectrum detection platform

165

166 2.3. Pineapple translucency degree assessment

167 After VIS/NIR spectrum sampling, pineapple translucency was assessed based on the
168 spectral data. Pineapples with different degrees of flesh translucency were not obviously
169 different from one another based on visual observation of the skin surfaces. Due to the lack of
170 an industrial standard for pineapple translucency degree assessment, a new pineapple
171 translucency degree assessment method was developed according to practical market
172 considerations. First, the pineapple is cut lengthwise into halves, which are further cut into 12
173 slices, and then tiled on a table. Second, the translucency degree is evaluated using three
174 categories: no translucency, slight translucency (edibleness and translucent area is up to 10 %
175 of the total sliced area), heavy translucency (edibleness and translucent area is more than 10 %
176 of the total sliced area). Third, the pineapple slices are turned over and checked using Step 2
177 again, and the most serious degree among the evaluation results was applied to represent
178 the translucency degree of the whole sample.

179

181 2.4. Data analysis

182 2.4.1. Analysis of the first batch of pineapples

183 The data from the first batch are applied for training the model. The scores from the
184 principal component analysis (PCA) (Wold et al., 1987) were applied for first checking the
185 classification effect and spatial distribution of samples in different pineapple translucency
186 categories. The Savitzky Golay (SG) filter (Press and Teukolsky, 1990) was applied to reduce

187 the jitter noise. The effect of SG is influenced by the order of polynomial and the size of the
188 smoothing window. Standard normal variate (SNV) (Barnes et al., 1989) was applied to reduce
189 the scattered noise due to the rough surface of the pineapple.

190 After applying SG and SNV as preprocessing, the successive projection algorithm (SPA)
191 (Araújo et al., 2001) was applied for feature extraction, in combination with the PCA and the
192 Euclidean distance (ED) (Danielsson, 1980) as follows. First, all features (transmissivity of
193 each wavelength after SG and SNV processing) were sorted by difference among samples
194 from large to small using SPA. Second, features were gradually added in order (sorted by SPA)
195 from two to the maximum and applied for PCA space classification, respectively; third, ED
196 was applied to calculate the distances between center points of different sample classes in PCA
197 classification-space, with the added feature retained if the ED increased (Xu et al., 2015; Xu et
198 al., 2014).

199 Partial least squares regression (PLSR) (Geladi and Kowalski, 1986) and probabilistic
200 neural network (PNN) (Specht, 1990) were applied for building the detection model. Holdout
201 cross validation was applied for data splitting to avoid overfitting. For model training based on
202 data of batch 1, to avoid inhomogeneity among translucency categories of traditional random
203 data selection of holdout cross validation, 38, 14, and 15 pineapple samples were randomly
204 selected from the no translucency, slight translucency, and heavy translucency categories,
205 respectively, were labeled as 1, 2 and 3, and were selected randomly from the first batch as the
206 calibration set, where the rest of the samples from the same batch were used as the validation
207 set. For PLSR, the factor number (FN) is the variable number selected after feature dimension
208 reduction as the input of modeling, which is the key parameter that affected the detection

209 accuracy, and was determined empirically in this study. In addition, due to the output of the
210 PLSR being decimal, the output was rounded-off to match the labeled value of the translucency
211 degree. For PNN, another key parameter, the Spread value (Ahmadlou and Adeli, 2010), is also
212 empirically determined. The integer output of the PNN can match the labeled translucency
213 degrees.

214 2.4.2. Analysis of the second batch of pineapples

215 The data from the second batch of pineapples were used for model updating. To
216 evaluate the adaptability of the detection model to different harvest times, the second batch
217 data (validation set) were applied to test the model which was built based on the first batch
218 data (calibration set). To further improve the adaptability of the detection model, three methods
219 were utilized for comparing the model updating effect, which included data correction, data
220 supplementation, and data correction + supplementation (Candolfi and Massart, 2000; Xie
221 and Ying, 2012). For data correction, a certain number of reference samples were selected from
222 the second batch, while the rest of the samples were used as the validation set. First, the
223 averages of the first batch sample SG and SNV processed spectral data and reference sample
224 SG and SNV processed spectral data of the second batch samples were calculated, to
225 compensate for the difference between averages for each validation samples. For data
226 supplementation, a certain number of reference samples were selected from the second batch,
227 and the rest were used for the validation set. The reference samples were added to the first
228 batch samples to re-train the detection model. For data correction + supplementation,
229 data correction was conducted to compensate for the differences in the averages for all the

230 second batch sample data (reference samples and validation samples), and corrected reference
231 samples were added to the first batch samples to re-train the detection model. To assess the
232 influence of the number of reference samples on the effect of model updating, 5-95 from the
233 second batch of pineapples were randomly selected as the model updating reference samples to
234 add into the first batch of pineapples (calibration set), with a step size of 5, where the rest of
235 the samples (validation set) were used as the validation samples to evaluate the model updating
236 effect.

237 2.4.3. Analysis of the third batch of pineapples

238 Data from the third batch of pineapples were applied for model testing (validation set).

239 The refined detection models with three updating methods and a different number of reference
240 samples added into the first batch of pineapples (calibration set) were applied for translucency
241 degree detection on the third batch of data. The results further verify the effectiveness of the
242 updated model.

244

245 3. Results and Discussion

246 3.1. Pineapple translucency degree distribution

247 The sample distribution in different translucency degrees for the three pineapple batches is
248 shown in Table 2. From the middle of April to the middle of May, 2021, the pineapple
249 translucency occurrence rate first increased and then declined, this same trend can also be
250 found in 2019 and 2020. In China, pineapple translucency only happens in April and May, the
251 season that a large number of pineapples are ready for harvest and marketing, due to high
252 rainfall followed by low rainfall in February (Pre-mature stage) in Zhanjiang, Guangdong,

253 China. Previous research also showed that PFT started to occur before the harvest and
 254 the occurrence rate increased with maturity development (Chen and Paull, 2000).
 255 However, PFT was only slightly related to the harvest season in Thailand, as it occurred
 256 the whole year (Joomwong and Sornsrivichai, 2006). The reason maybe that Thailand in a
 257 tropical area with a high temperature, and intense illumination almost all year.

258 Table 2 Translucency degree distribution of three batches of pineapples

Batch	No translucency		Slight translucency		Heavy translucency		Sum number
	Number	Proportion (%)	Number	Proportion (%)	Number	Proportion (%)	
1	56	56.0	21	21.0	23	23.0	100
2	24	24.0	31	31.0	45	45.0	100
3	38	42.2	24	26.7	28	31.1	90
Sum	118	40.7	76	26.2	96	33.1	290

260

261 3.2. Evaluation of pineapple translucency detection model

262 3.2.1. Classification using raw spectrum data

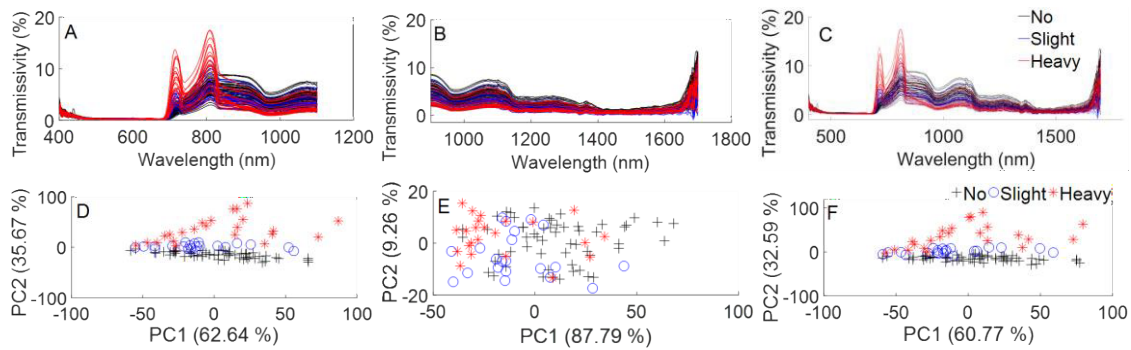
263 Fig. 2(A-C) shows the raw spectrum data from the first batch of pineapples at 400-1100
 264 nm, 900-1700 nm and 400-1700 nm, respectively. As seen, more jitter noise can be observed in
 265 the NIR spectrum, especially over 1100 nm. The reason is mainly due to the degradation of
 266 degradation of optical energy with increasing wavelength, where the NIR spectrum can be
 267 more easily absorbed by water while transmitting the fruit than the VIS wavelengths (Liu et al.,
 268 2020). The more translucent fruit has higher transmissivity in the VIS spectrum but lower
 269 in the NIR spectrum, because translucency happens with increased water content in the

270 intercellular spaces, thus, VIS transmits better than NIR spectrum.

271 Pineapple translucency degrees can be classified in three categories based on the PC1 and PC2
272 of the visible and NIR spectrum within 400-1100 nm (Fig. 2(D)). However, the boundary of
273 each class overlaps with the others, and the clustering performance is poor. For NIR spectrum
274 in 900-1700 nm, the three separate pineapple translucency degrees cannot be
275 differentiated as shown in Fig. 2(E). The occurrence of pineapple translucency is accompanied
276 by changes of flesh color, texture, and other components e.g. sugar accumulation, water
277 content increase, and sugar fermentation (Chen and Paull, 2000). Optically, the visible
278 spectrum and the NIR spectrum are sensitive to color and component (with
279 hydrogen-containing groups) changes (Arendse et al., 2018), respectively, meanwhile both VIS
280 and NIR spectrums are sensitive to flesh texture (Alhamdan et al., 2019). The reason that
281 visible and NIR spectrum within 400-1100 nm have better translucency classification than
282 the NIR spectrum within 900-1700 nm is that translucency involves both flesh color and
283 component changes, to which the visible and NIR spectrum is more sensitive and has a relative
284 high SNR. On the contrary, the NIR spectrum is quite sensitive to component change and a
285 relatively low SNR (Liang et al., 2009). In addition, the classification result using the
286 combined spectrum of 400-1700 nm in Fig. 2(F) is quite similar to those using visible and
287 NIR spectrum only, thus it can be inferred that the primary and most useful information for
288 translucency degree classification is from visible and NIR spectrum within 400-900 nm. In
289 addition, the rough surface brings scattered noise for spectrum detection. Thus, the
290 nondestructive detection of pineapple translucency is too difficult to use methods for fruit

291 internal quality inspection, and requires an improvement in method, from platform to signal
292 preprocessing to modeling.

293



293

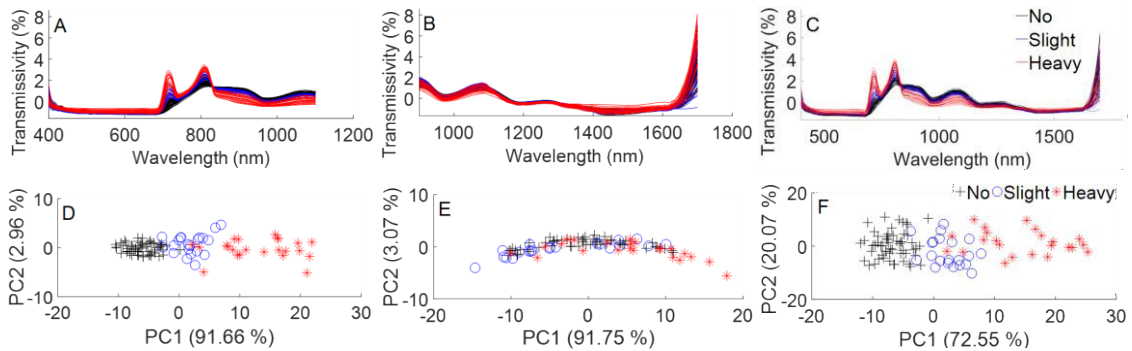
294 **Fig. 2.** Raw spectrum data (top) and the PCA space transluency classification results (bottom)
295 of the first batch pineapple based on wavelengths of 400-1100 nm (A, D), 900-1700 nm (B, E),
296 and 400-1700 nm (C, F).

297

298 3.2.2. Classification based on denoised spectrum

299 Considering that the jitter noise in the spectrum may affect the classification, the
300 classification results were evaluated under different SG models for smoothing, where 3 orders
301 23 points SG, 3 orders 41 points SG, and 3 orders 41 points SG were applied for denoising the
302 spectrums in 400-1100 nm, 900-1700 nm, and 400-1700 nm, respectively for their best
303 performance in the experiments. In addition, due to the highly rough surface of the pineapples,
304 scattering noise is unavoidable in sampling the spectral signal. Thus, SNV was applied to
305 suppress the scattering noise after SG based de-noising, see in Fig. 3(A-C). After applying SG
306 and SNV for denoising, the PC1 and PC2 obtained from different spectrums is visualized,
307 where the results from 400-1100 nm, 900-1700 nm, and 400-1700 nm are shown in Fig. 3(D-F),
308 respectively. The clustering performance is largely improved, and the overlapping is

309 largely reduced when compared to the results from the raw spectral data shown in Fig. 2(D-
 310 F). Three translucency degrees are easily distinguishable using 400-1100 nm and 400-1700
 311 nm spectrums, but not using the 900-1700 nm spectrum. However, there is still some
 312 overlapping between different translucency classes.



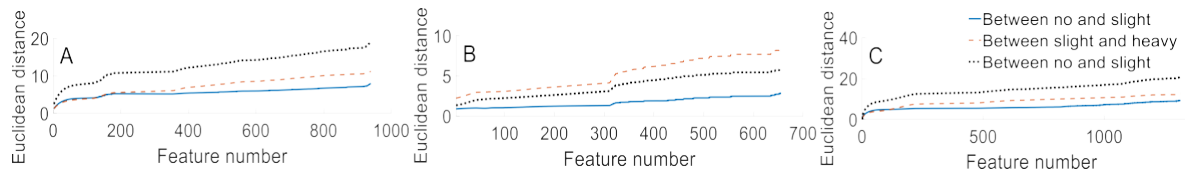
313
 314 **Fig. 3.** Raw data (top) and PCA space translucency classification (bottom) of the first batch
 315 pineapples after applying SG and SNV for denoising the spectrum of 400-1100 nm (A, D),
 316 900-1700 nm (B, E), and 400-1700 nm (C, F), respectively.

317

318 3.2.3. Feature selection and detection model training

319 Fig. 4 shows the Euclidean distance changes between different translucency classes in the
 320 PCA space (composed of PC1 and PC2) while gradually increasing the features in order
 321 (ordered by SPA). The effectiveness of this method has been shown in previous research
 322 (Xu et al., 2015; Xu et al., 2014). Even the external appearance rarely changed with the
 323 occurrence of translucency, however, the color, cell structure, and material composition of
 324 internal flesh are apparently different, where all the wavelengths from 400 to 1700 nm can
 325 contribute positively to translucency degree detection. In this study, there are 940 and 956 data
 326 points in total for 400-1100 nm and 900-1700 nm spectrums, respectively. The test results have

327 shown that these data can be calculated to output the translucency degree within 0.001 sec for
328 detection using SG, SNV and PLSR detection, or 0.06 sec for PNN with SG and SNV on a
329 Lenovo Laptop T14 (Intel i7 CPU, 16.0 GB RAM). Thus, the feature number can satisfy the
330 requirement of real-time detection in industrial applications.



331
332 **Fig. 4.** SPA + PCA + ED contribution analysis of spectral feature from (A) 400 to 1100 nm, (B)
333 900 to 1700 nm, and (C) 400 to 1700 nm.

334
335 Table 3 shows the results of pineapple translucency degree detection using PLSR and PNN,
336 based on different spectra after de-noising with SG and SNV. Pineapple translucency degree can
337 be accurately detected using the 400-1100 nm spectra and 400-1700 nm spectra, but not the
338 900-1700 nm spectrum. In addition, 400-1100 nm and 400-1700 nm spectra produced the same
339 detection accuracy in the validation set. In general, PNN has better results than PLSR in
340 translucency detection, especially for the validation set. This is because the kernel algorithm of
341 PNN has a stronger capability than the linear regression used in PLSR, especially in modeling
342 the nonlinear characteristics of translucency degree, as seen with the non-linearly separable
343 boundaries between different translucency classes in Fig. 2(D-F). Considering further the
344 relatively low cost of the QE pro for 400-1100 nm compared to the NIR QUEST for 900-1100
345 nm, the optimal pineapple translucency detection method would use 400-1100 nm spectrum
346 along with SG and SNV for de-noising and PNN for classification.

347 However, considering the stability in practical use, the testing of the NIR spectrum is still

348 needed for comparison in future experiments.

349 Table 3 PLSR and PNN based translucency degree detection results using different spectrums
 350 with holdout cross validation data splitting

	Wavelength (nm)	Parameter		Calibration set (67 of the first batch)				Validation set (34 of the first batch)			
				Parameter				Parameter			
		FN	Spread	No	Slight	Heavy	Total	No	Slight	Heavy	Total
	400-1100	11	-	100.0	100.0	93.3	98.5	94.74	100.0	62.5	88.24
PLSR	900-1700	11	-	89.5	73.3	66.7	80.6	73.7	57.14	25.0	58.8
	400-1700	14	-	100.0	100.0	100.0	100.0	84.2+	100.0	93.3	88.24
	400-1100	-	1.2	100.0	100.0	93.3	98.5	100.0	85.7	75.0	91.2
PNN	900-1700	-	0.1	100.0	100.0	100.0	100.0	73.7	28.6	62.5	62.0
	400-1700	-	0.2	100.0	100.0	100.0	100.0	100.0	85.7	75.0	91.2

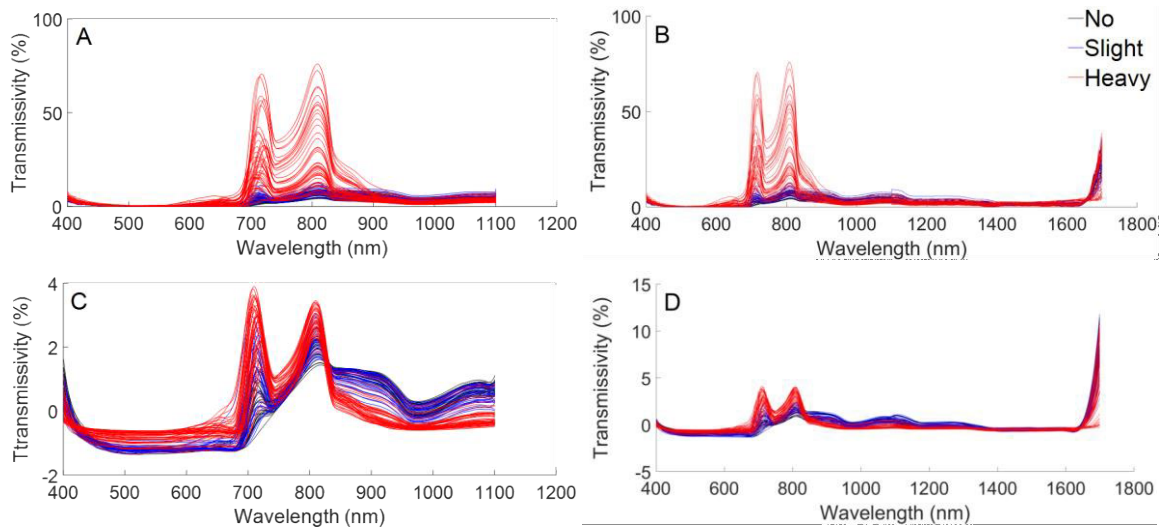
351

352 3.3. Model updating using the second batch of pineapple samples

353 3.3.1. Necessity test of model updating

354 Fig. 5(A-B) show the raw spectral data of the second batch of pineapples in 400-1100 nm,
 355 and 400-1700 nm, respectively, and their de-noised versions using SG and SNV are shown in
 356 Fig. 5(C-D). Compared to the spectral data of the first batch, the second batch has a similar
 357 spectral profile, but higher transmissivity in VIS/NIR spectrum and lower transmissivity in
 358 NIR spectrum. This is due to the second batch having more serious translucency, as shown in
 359 Table 2, which has led to a lower density (or less blockage for VIS/NIR spectrum) and higher
 360 water content (more absorption for NIR spectrum) in the flesh.

361



362

363 **Fig. 5.** Raw spectrum data (A, B) and denoised data using SG and SNV (C, D) of the second
364 batch of pineapple samples using 400-1100 nm spectrum (A, C), and 400-1700 nm spectrum
365 (B, D), respectively.

366

367 To further validate the efficacy of the trained optimal detection method derived from the first
368 batch of pineapples, the second batch of pineapples were tested using this model. In addition,
369 the samples were also increased for training the model from 67 to 100, all from the first batch
370 of samples, the model was then tested using the 100 samples from the second batch, and the
371 results are summarized in Table 4. As seen, SG + SNV + PNN still produces the best results
372 for the validation set, especially with the VIS/NIR spectrum in the 400-1100 nm spectrum,
373 where the 400-1700 nm spectrum seems unfeasible as it can be easily affected by external
374 disturbance e.g. sample difference. Thus, 400-1700 nm spectra slightly improved the
375 detection accuracy on the calibration set compared to 400-1100 nm spectra (Table 3),
376 which has the risk of lowering the detection accuracy with the addition of interference

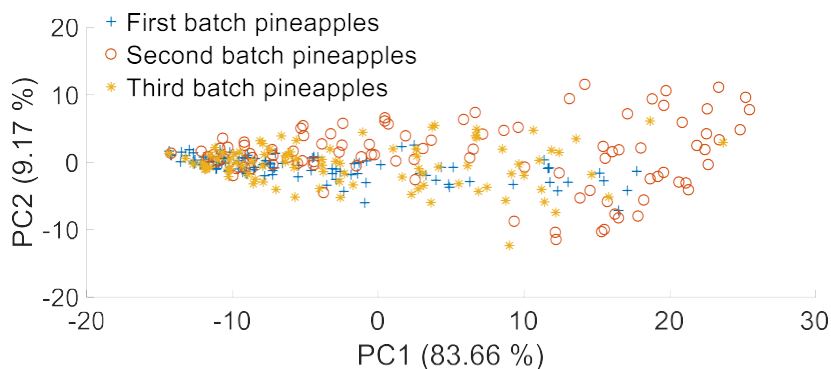
377 factors like sample difference (Table 4). Thus, 400-1100 nm spectra already contained
 378 major information for pineapple translucency detection, 1100-1700 nm supplied minimal
 379 extra useful information compared to 400-1100 nm spectra. In addition, the previous research
 380 also proved multi-information fusion had the potential to both increase and reduce detection
 381 accuracy (Xu et al., 2019). Thus, 400-1100 nm is a low cost and efficient way for the
 382 nondestructive detection of pineapple translucency. Additionally, increasing training samples
 383 can improve the detection accuracy on the validation set, but not on the calibration set, as fewer
 384 training samples will likely result in over fitting. As the testing was carried out using a
 385 different batch of samples, the detection accuracy decreased from 91.2 % to 70 % when
 386 compared to testing on the same batch of samples. Thus, model updating is necessary for model
 387 adaptation improvement.

388 Table 4 Results from first pineapple batch detection model used to test the second pineapple
 389 batch with holdout cross-validation

	Wavelength (nm)	Modeling sample number	Calibration set (the whole first batch) (%)				Validation set (the whole second batch) (%)			
			No	Slight	Heavy	Total	No	Slight	Heavy	Total
PLSR	400-1100	67	100.0	100.0	93.3	98.5	91.7	19.4	22.2	38.0
		100	100.0	77.8	91.3	92.0	91.7	25.8	37.8	47.0
	400-1700	67	100.0	100.0	100.0	100.0	95.8	6.45	37.8	43.0
		100	96.0	85.2	87.0	91.0	25.0	71.0	62.2	56.0
PNN	400-1100	67	100.0	100.0	93.3	98.5	50.0	45.2	91.1	67.0
		100	100.0	77.8	100.0	94.0	62.5	45.2	91.2	70.0
	400-1700	67	100.0	100.0	100.0	100.0	100.0	3.3	15.6	32.0
		100	100.0	100.0	100.0	100.0	100.0	6.45	17.8	34.0

392 3.3.2. Translucency detection model updating

394 The PCA score plot clearly shows the almost original distribution of samples in a same
395 space. To visualize the difference among these three batches of pineapples, the PC1 and
396 PC2 of each SG and SNV processed sample data is shown in Fig. 6 for comparison. Obviously,
397 the first batch cannot cover the other two, which explains the low validation accuracy when
398 testing the second batch of pineapples using the detection model trained on the first batch of
399 pineapples. Model updating research is an essential step to move the application of
400 spectroscopy forward. Thus, model updating is applied to tackle this problem.



401

402 **Fig. 6.** PCA score plot of the three batches of pineapples

403

404 Data correction, data supplementation, and the combination of these two schemes were
405 applied to determine the optimal model updating strategy to tackle the low detection accuracy
406 issue caused by the differences between the samples. Specifically, some of the second batch
407 samples were incrementally taken as references to update the trained model derived from the first
408 batch of pineapple samples. The model updating results are shown in Fig. 7. The detection
409 accuracy on the calibration set of all three model-updating methods increased while adding
410 additional reference samples, which reached over 96 % after five samples (Fig. 7(A)). For the

411 validation set, not surprisingly, the detection accuracy also kept improving (Fig. 7(B)). However,

412 the detection accuracy stability using the data supplementation scheme seems better than the

413 other two methods. With the data supplemented by 40 reference samples from the second batch

414 of pineapples, the detection accuracy on the validation set can be improved from 70 % to

415 80 %, which is satisfactory for the accurate detection of pineapple translucency degree. For

416 the three model updating methods using 85 reference samples from the second batch of

417 pineapples, the detection accuracy of the validation sets can all achieve 100 %. Both data

418 supplementation (Schimleck et al., 2006) and data correlation (Yao et al., 2010) were proven

419 useful for the different targets' detection model updating. Xie et al. found the model updating

420 effect of data correlation was better than data supplementation in tomato quality detection (Xie

421 and Ying, 2012). Thus, there is no one model updating method which fits all detection targets,

422 due to the specifics of different agricultural products. In addition, a data correlation +

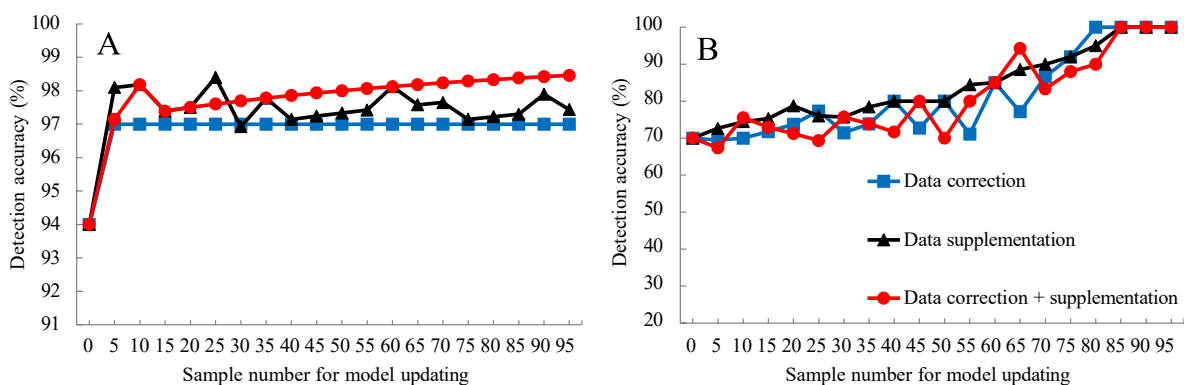
423 supplementation method was proposed in this study, and that model's updating effect was worse

424 than the data supplementation model's effect. However, data correlation + supplementation

425 may be the optimal model updating effect for quality detection of other targets, and future

426 research is required to confirm this. A third batch of pineapples is needed to further validate the

427 efficacy of the three model updating methods.



429

430 **Fig. 7.** Results of model updating on the calibration set (A) and the validation set (B) by
431 progressively increasing samples from the second batch.

432

433 3.4. Testing on the updated model using the third batch of pineapples

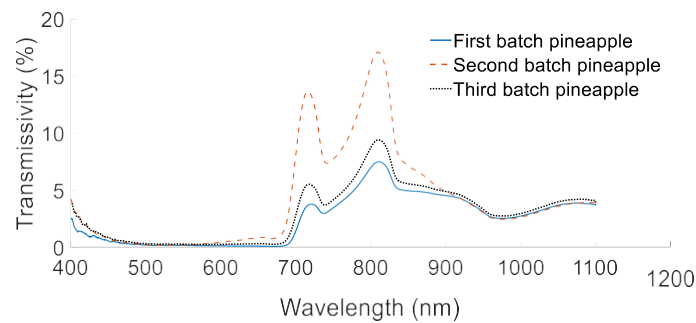
434 Before testing the accuracy of the updated model using the third batch of pineapples, the

435 average spectra of the first, second, and third batches of pineapples were compared in Fig. 8.

436 The second batch of pineapples shows the highest transmissivity, followed by the third and the

437 first batches. It can also be further confirmed that, pineapples with more serious translucency

438 tend to have higher spectral transmissivity.



440

441 **Fig. 8.** Average of raw spectrums of the first, second and third batch of pineapples

442

443 Ninety pineapple samples in the third batch were harvested to further validate the

444 efficacy of the updated models, using the three model updating schemes for detection of the

445 degree of pineapple translucency. As shown in Fig. 9(A), the data correction based model

446 updating method degrades the validation accuracy with an increasing number of references

447 samples. The reason for this is that each pineapple batch should be more or less different from

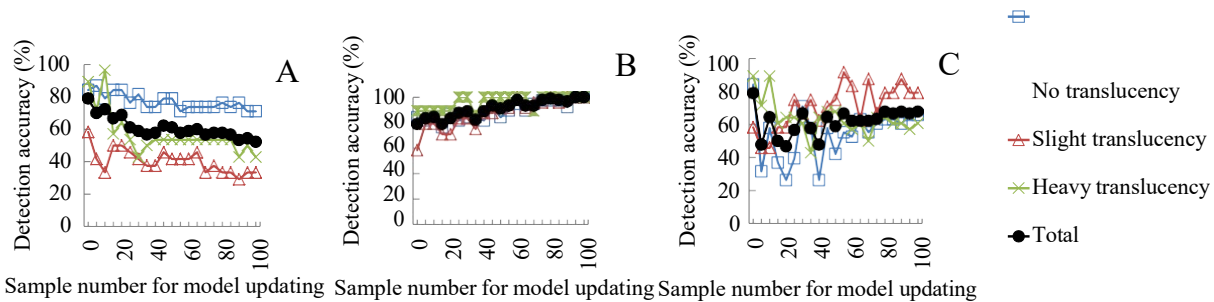
448 the others, thus the reference samples of the second batch cannot represent the validation

449 samples from the third batch. In other words, a data correction based model updating method is

450 only suitable for detection within the same batch of training and testing samples. For the
451 data supplementation based model updating method, where the pre-trained model was retrained
452 using the second batch of samples, it can still achieve a very high accuracy for the validation
453 set of the third batch of pineapples for pineapple translucency detection, see in Fig. 9(B). When
454 40 or more reference samples were added for model updating, the detection accuracies of the
455 total and each individual translucency degree can be at least 80 %, and nearly 100 % when 95
456 reference samples were added for model updating. Thus the supplementing of the second batch
457 of samples with the first batch can largely improve the data set multiformity to cover the
458 characteristics of the third batch samples. In addition, combining data correction and data
459 supplementation for model updating also shows a poor ability in improving the detection
460 accuracy for practical application, see in Fig. 9(C), and the updating effect on model accuracy on
461 the validation set of the third batch of pineapples seemed unstable with an increasing number of
462 reference samples from the second batch of pineapples for. As a result, data supplementation is
463 found to be the most effective and robust model updating scheme for the detection of
464 pineapple translucency. As shown in Fig. 6, and 8, it can be seen that the first two batches
465 of pineapples can cover most of the characteristics of the third batch. Therefore, the translucency
466 of the third batch can be successfully detected by using the model based on the first two
467 batches of pineapple. Thus, this study provided an optimal VIS/NIR detection platform
468 parameter, and demonstrated the efficiency of SG and SNV for signal preprocessing, and PNN
469 for modeling, for the nondestructive detection of pineapple translucency. Compared to other
470 potential methods, such as acoustic impulse-response technique, the noise interference problem
471 of VIS/NIR spectroscopy, which is more stable and promising for industrial

472 applications, can be efficiently solved by model updating.

473



476 **Fig. 9.** Detection results on the third batch of pineapples with different model updating
477 approaches including data correction (A), data supplementation (B), and the combined scheme
478 (C).

479

480

481 **4. Conclusion**

482 VIS/NIR spectroscopy coupled with data analysis and machine learning was used for
483 nondestructive detection of PFT. The developed low-cost detection platform can meet
484 industrial requirements and work on assembly lines for real-time operations, and the optimal
485 parameters can be empirically determined for the best efficacy.

486 In this system, SG and SNV were found to be useful in removing the jitter noise caused by low
487 SNR of the large fruit size and the scattering noise caused by the irregular and rough surface of
488 the pineapple. Accordingly, SG and SNV can help to improve the data clustering performance
489 for the classification of pineapple translucency in the PCA space for a reduced dimension of
490 the data. The spectral data from VIS/NIR wavelengths of 400-1100 nm is found particularly
491 useful. Also, PNN produced better results than PLSR in solving nonlinear classification

492 problems of pineapple translucency degrees. To tackle the sample difference of training and
493 validation data, data supplementation is found to produce particularly good results compared to
494 data correction or the combination of these two schemes for model updating. Therefore, the
495 optimal roadmap for pineapple translucency detection in the industry is a recommendation
496 to adopt the 400-1100 nm spectrum data, followed by SG and SNV based de-noising, PNN
497 based data classification, and data supplementation for model updating. The proposed
498 approach can be used as a rapid, nondestructive, and cost-effective framework to detect
499 pineapple translucency. It can help to guarantee the quality of fruit sent to market, to alert
500 pineapple processors around the world to the possible need for post harvest treatment, and
501 to improve the market competitiveness.

503

504 **Funding**

505 This study has no financial relationship with the organization that sponsored the research.

506

507 **Declaration of conflicts of interest statement**

508 The authors declare no conflicts of interest.

509

510 **Acknowledgements**

511 The authors acknowledge the financial support of Laboratory of Lingnan Modern
512 Agriculture Project (NT2021009), Natural Science Foundation of Guangdong Province
513 (2021A1515010834), the Special fund for rural revitalization of Guangdong Province
514 (403-2018-XMZC-0002-90), National Natural Science Foundation of China (31901404), New
515 Developing Subject Construction Program of Guangdong Academy of Agricultural Science
516 (Project No. 202134T), the Presidential Foundation of Guangdong Academy of Agricultural
517 Science (Project No. 202034), Talent Training Program of Guangdong Academy of
518 Agricultural Science (R2020PY-JJX020), Young Talent Support Project of Guangzhou
519 Association for Science and Technology, and Provincial Agricultural Science and Technology
520 Innovation and Extension System Construction Project (2020KJ256). USDA is an equal
521 opportunity provider and employer.

522

523 **References**

- 524 Adedeji, A.A., Ekramirad, N., Rady, A., Hamidisepehr, A., Donohue, K.D., Villanueva, R.T.,
525 Parrish, C.A., Li, M., 2020. Non-destructive technologies for detecting insect infestation in
526 fruits and vegetables under postharvest conditions: A critical review. *Foods* 9 (7), 927.
527 <https://doi.org/10.3390/foods9070927>
- 528 Adetunji, C.O., Fawole, O. B., Arowora, K. A., Nwaubani, S.I., Ajayi, E.S., Oloke, J.K.,
529 Majolag, 2012. Effects of edible coatings from Aloe vera gel on quality and postharvest
530 physiology of *Ananas comosus* (L.) fruit during ambient storage. *Global Journal of Science*
531 *Frontier Research Bio-Tech & Genetics* 12(5), 39-43.
532 <https://journalofscience.org/index.php/GJSFR/article/view/702>
- 533 Ahmadlou, M., Adeli, H., 2010. Enhanced probabilistic neural network with local decision
534 circles: A robust classifier. *Integr. Comput.-Aid. E.* 17(3), 197-210.
535 <https://doi.org/10.3233/ICA-2010-0345>
- 536 Alhamdan, A.M., Fickak, A., Atia, A.R., 2019. Evaluation of sensory and texture profile
537 analysis properties of stored Khalal Barhi dates nondestructively using Vis/NIR
538 spectroscopy. *J. Food Process Eng.* 42 (6), e13215. <https://doi.org/10.1111/jfpe.13215>
- 539 Araújo, M.C.U., Saldanha, T.C.B., Galvao, R.K.H., Yoneyama, T., Chame, H.C., Visani, V.,
540 2001. The successive projections algorithm for variable selection in spectroscopic
541 multicomponent analysis. *Chemometr. Intell. Lab.* 57 (2), 65-73.
542 [https://doi.org/10.1016/S0169-7439\(01\)00119-8](https://doi.org/10.1016/S0169-7439(01)00119-8)
- 543 Arendse, E., Fawole, O.A., Magwaza, L.S., Nieuwoudt, H., Opara, U.L., 2018. Fourier

544 transform near infrared diffuse reflectance spectroscopy and two spectral acquisition modes
545 for evaluation of external and internal quality of intact pomegranate fruit. *Postharvest Biol.*
546 *Tec.* 138, 91-98. <https://doi.org/10.1016/j.postharvbio.2018.01.001>

547 Barnes, R.J., Dhanoa, M.S., Lister, S.J., 1989. Standard normal variate transformation and
548 de-trending of near-infrared diffuse reflectance spectra. *Appl. Spectrosc.* 43 (5), 772-777.
549 <https://doi.org/10.1366/0003702894202201>

550 Candolfi, A., Massart, D.L., 2000. Model updating for the identification of NIR spectra from a
551 pharmaceutical excipient. *Appl. Spectrosc.* 54 (1), 48-53.
552 <https://doi.org/10.1366/0003702001948105>

553 Cano Reinoso, D.M., 2021. Management Protection on Quality Determination of Flesh
554 Translucency and Fruit Collapse Disease on Indonesian MD2 Pineapple: Universitas
555 Jenderal Soedirman. <http://repository.unsoed.ac.id/11056/>

556 Chen, C., 1999. Effects of fruit temperature, calcium, crown and sugar-metabolizing enzymes
557 on the occurrence of pineapple fruit translucency University of Hawai'i at Manoa.
558 [https://www.proquest.com/openview/71e71b7f4d240c048f45ea343d3fe944/1?pq-origsite=g](https://www.proquest.com/openview/71e71b7f4d240c048f45ea343d3fe944/1?pq-origsite=scholar&cbl=18750&diss=y)
559 [scholar&cbl=18750&diss=y](https://www.proquest.com/openview/71e71b7f4d240c048f45ea343d3fe944/1?pq-origsite=scholar&cbl=18750&diss=y)

560 Chen, C., Paull, R.E., 2000. Sugar metabolism and pineapple flesh translucency. *J. Am. Soc.*
561 *Hortic. Sci.* 125 (5), 558-562. <https://doi.org/10.21273/JASHS.125.5.558>

562 Cruz, S., Guerra, R., Brazio, A., Cavaco, A.M., Antunes, D., Passos, D., 2021. Nondestructive
563 simultaneous prediction of internal browning disorder and quality attributes in 'Rocha'
564 pear (*Pyrus communis* L.) using VIS-NIR spectroscopy. *Postharvest Biol. Tec.* 179, 111562.

565 <https://doi.org/10.1016/j.postharvbio.2021.111562>

566 Danielsson, P., 1980. Euclidean distance mapping. *Computer Graphics and image processing*

567 14 (3), 227-248. [https://doi.org/10.1016/0146-664X\(80\)90054-4](https://doi.org/10.1016/0146-664X(80)90054-4)

568 Duprat, F., Grotte, M., Piétri, E., Loonisa, D., Studman, C.J., 1997. The acoustic impulse

569 response method for measuring the overall firmness of fruit. *Journal of agricultural*

570 *engineering research*. 66 (4), 251-259. <https://doi.org/10.1006/jaer.1996.0143>

571 Fassinou Hotegni, V.N., Lommen, W.J.M., van der Vorst, J.G.A.J., Agbossou, E.K., Struik,

572 P.C., 2014. Bottlenecks and opportunities for quality improvement in fresh pineapple

573 supply chains in Benin. *International Food and Agribusiness Management Review*

574 17(1030-2016-83025), 139-170. <https://doi.org/10.22004/ag.econ.183473>

575 Geladi, P., Kowalski, B.R., 1986. Partial least-squares regression: A tutorial. *Anal. Chim. Acta*

576 185, 1-17. [https://doi.org/10.1016/0003-2670\(86\)80028-9](https://doi.org/10.1016/0003-2670(86)80028-9)

577 Haff, R.P., Slaughter, D.C., Sarig, Y., Kader, A., 2006. X - ray assessment of translucency in

578 pineapple. *J. Food Process. Pres.* 30 (5), 527-533.

579 <https://doi.org/10.1111/j.1745-4549.2006.00086.x>

580 Jie, D., Xuan, W., 2018. Review on the recent progress of non-destructive detection technology

581 for internal quality of watermelon. *Computers & Electronics in Agriculture* 151, 156-164.

582 <https://doi.org/10.1016/j.compag.2018.05.031>

583 Joomwong, A., Sornsrivichai, J., 2006. Impact of cropping season in northern Thailand on the

584 quality of smooth cayenne pineapple. II. Influence on physico-chemical attributes. *Int. J.*

585 *Agric. Biol.* 8(6), 330-336. <https://www.researchgate.net/publication/228728029>

586 Korres, A.M.N., Ventura, J.A., Fernandes, P.M.B., 2010. First report of bacterium and yeasts
587 associated with pineapple fruit collapse in Espírito Santo State, Brazil. *Plant Dis.* 94(12),
588 1509-1509. <https://doi.org/10.1094/PDIS-04-10-0276>

589 Li, J.L., Sun, D.W., Cheng, J.H., 2016. Recent advances in nondestructive analytical
590 techniques for determining the total soluble solids in fruits: A review. *Compr. Rev. Food*
591 *Sci. F.* 15 (5), 897-911. <https://doi.org/10.1111/1541-4337.12217>

592 Liang, L., Liu, Z., Yang, M., Zhang, Y., Wang, C., 2009. Discrimination of variety and
593 authenticity for rice based on visual/near infrared reflection spectra. *J. Infrared Millim. W.*
594 *28* (5), 353-356. <https://doi.org/10.3724/SP.J.1010.2009.00353>

595 Liu, Z., Chen, S., Yu, T., Ma, G., Huang, X., Yu, C., Lin, H., 2020. Effects of sunlight on eye.
596 *International Eye Science* 20 (3), 191-196. <https://doi.org/10.18240/ier.2021.01.10>

597 Lu, R., Van Beers, R., Saeys, W., Li, C., Cen, H., 2020. Measurement of optical properties of
598 fruits and vegetables: A review. *Postharvest Biol. Tec.* 159, 111003.
599 <https://doi.org/10.1016/j.postharvbio.2019.111003>

600 Mandal, D., Vanlalawmpuia, C., 2020. Impact of postharvest use of essential oils on quality
601 and shelf life of Indian pineapple. *Journal of Postharvest Technology* 8(3), 96-105.
602 <https://www.researchgate.net/publication/350190874>

603 Montero-Calderón, M., Rojas-Graü, M.A., Martín-Belloso, O., 2008. Effect of packaging
604 conditions on quality and shelf-life of fresh-cut pineapple (*Ananas comosus*). *Postharvest*
605 *Biol. Tec.* 50(2-3), <https://doi.org/10.1016/j.postharvbio.2008.03.014>

606 Murai, K., Chen, N.J., Paull, R.E., 2021. Pineapple crown and slip removal on fruit quality and

607 translucency. *Sci. Hortic.-Amsterdam* 283, 110087.
608 <https://doi.org/10.1016/j.scienta.2021.110087>

609 Naik, S., Patel, B., 2017. Machine vision based fruit classification and grading-a review.
610 *International Journal of Computer Applications* 170 (9), 22-34.
611 <https://doi.org/10.5120/ijca2017914937>

612 Pahlawan, M., Wati, R.K., Masithoh, R.E., 2021. Development of a low-cost modular VIS/NIR
613 spectroscopy for predicting soluble solid content of banana, *IOP Conference Series: Earth
614 and Environmental Science* (Vol. 644, pp. 12047): IOP Publishing.
615 <https://doi.org/10.1088/1755-1315/644/1/012047>

616 Paull, R.E., Chen, N.J., 2013. Pineapple translucency and chilling injury in new low-acid
617 hybrids, II Southeast Asia Symposium on Quality Management in Postharvest Systems
618 1088 (pp. 61-66). <https://doi.org/10.17660/ActaHortic.2015.1088.5>

619 Paull, R.E., Reyes, M.E., 1996. Preharvest weather conditions and pineapple fruit translucency.
620 *Sci. Hortic.-Amsterdam* 66 (1-2), 59-67. [https://doi.org/10.1016/0304-4238\(96\)00905-3](https://doi.org/10.1016/0304-4238(96)00905-3)

621 Press, W.H., Flannery, B.P., Teukolsky, S.A., Vetterling, W.T., 1990. Savitzky - Golay
622 smoothing filters. *Computers in Physics* 4 (6), 669-672. <https://doi.org/10.1063/1.4822961>

623 Py, C., Lacoeyllhe, J., Teisson, C., 1987. *The pineapple: Cultivation and uses* Paris: GP
624 Maisonneuve & Larose. <http://hdl.handle.net/10524/55419>

625 Schimleck, L.R., Kube, P.D., Raymond, C.A., Michell, A.J., French, J., 2006. Extending near
626 infrared reflectance (NIR) pulp yield calibrations to Newsites and species. *J. Wood Chem.
627 Technol.* 26 (4), 299-311. <https://doi.org/10.1080/02773810601076683>

628 Shi, H., Zhang, M., Adhikari, B., 2018. Advances of electronic nose and its application in fresh
629 foods: A review. *Crit. Rev. Food Sci.* 58 (16), 2700-2710.
630 <https://doi.org/10.1080/10408398.2017.1327419>

631 Specht, D.F., 1990. Probabilistic neural networks. *Neural Networks* 3 (1), 109-118.
632 [https://doi.org/10.1016/0893-6080\(90\)90049-Q](https://doi.org/10.1016/0893-6080(90)90049-Q)

633 Wang, H., Peng, J., Xie, C., Bao, Y., He, Y., 2015. Fruit quality evaluation using spectroscopy
634 technology: A review. *Sensors-Basel* 15 (5), 11889-11927.
635 <https://doi.org/10.3390/s150511889>

636 Wold, S., Esbensen, K., Geladi, P., 1987. Principal component analysis. *Chemometr. Intell.*
637 *Lab.* 2 (1-3), 37-52. [https://doi.org/10.1016/0169-7439\(87\)80084-9](https://doi.org/10.1016/0169-7439(87)80084-9)

638 Xie, L., Ying, Y., 2012. Calibration model maintenance method for transgenic tomato
639 discriminant. *Journal of Jiangsu University (Natural Science Edition)* 33(5), 538-542.
640 <https://doi.org/10.3969/j.issn.1671-7775.2012.05.009>

641 Xu, S., Lu, H., Ference, C., Qiu, G., Liang, X., 2020. Rapid nondestructive detection of water
642 content and granulation in postharvest “shatian ” pomelo using Visible/Near-Infrared
643 spectroscopy. *Biosensors* 10 (4), 41. <https://doi.org/10.3390/bios10040041>

644 Xu, S., Lu, H., Liang, X., Qiu, G., Lin, W., 2021. Effect of artificial ripening on postharvest
645 pineapple fruit quality and its recognition by spectroscopy. *Food Science* 42 (9), 192-198.
646 <https://doi.org/10.7506/spkx1002-6630-20200513-144>

647 Xu, S., Lu, H., Zhou, Z., Lü, E., Jiang, Y., 2015. Identification for guava mechanical damage
648 based on combined hyper-spectrometer and electronic nose. *Transactions of the Chinese*

649 Society for Agricultural Machinery 46 (7), 214-219.
650 <https://doi.org/10.6041/j.issn.1000-1298.2015.07.031>

651 Xu, S., Sun, X., Lu, H., Zhang, Q., 2019. Detection of type, blended ratio, and mixed ratio of
652 pu 'er tea by using electronic nose and Visible/Near infrared spectrometer. *Sensors-Basel* 19
653 (10), 2359. <https://doi.org/10.3390/s19102359>

654 Xu, S., Zhou, Z., Lu, H., Luo, X., Lan, Y., 2014. Improved algorithms for the classification of
655 rough rice using a bionic electronic nose based on PCA and the Wilks distribution.
656 *Sensors-Basel* 14 (3), 5486-5501. <https://doi.org/10.3390/s140305486>

657 Yao, S., Wu, G., Jiang, Y., Fu, X., Lü, H., Su, M., Pu, J., 2010. Extending hemicelluloses
658 content calibration of acacia spp using nir to new sites. *Spectrosc. Spect. Anal.* 30 (5),
659 1206-1209. [https://doi.org/10.3964/j.issn.1000-0593\(2010\)05-1206-04](https://doi.org/10.3964/j.issn.1000-0593(2010)05-1206-04)

660 Zhang, Y., Chen, Y., Wu, Y., Cui, C., 2021. Accurate and nondestructive detection of apple
661 brix and acidity based on visible and near-infrared spectroscopy. *Appl. Optics* 60 (13),
662 4021-4028. <https://doi.org/10.1364/AO.423994>.

663